

# Mapping the spectrum of 3D communities in human chromosome conformation capture data

Sang Hoon Lee<sup>1,\*</sup>, Yeonghoon Kim<sup>2</sup>, Sungmin Lee<sup>3</sup>, Xavier Durang<sup>4</sup>, Per Stenberg<sup>5</sup>,  
Jae-Hyung Jeon<sup>2,†</sup>, Ludvig Lizana<sup>6,‡</sup>

**1** Department of Liberal Arts, Gyeongnam National University of Science and Technology, Jinju 52725, Korea

**2** Department of Physics, Pohang University of Science and Technology, Pohang 37673, Korea

**3** Department of Physics, Korea University, Seoul 02841, Korea

**4** Department of Physics, University of Seoul, Seoul 02504, Korea

**5** Department of Ecology and Environmental Science (EMG), Umeå University, Umeå 90187, Sweden

**6** Integrated Science Lab, Department of Physics, Umeå University, Umeå 90187, Sweden

\*lshlj82@gntech.ac.kr

†jeonjh@postech.ac.kr

‡ludvig.lizana@umu.se

## Abstract

Several experiments show that the three dimensional (3D) organization of chromosomes affects genetic processes such as transcription and gene regulation. To better understand this connection, researchers developed the Hi-C method that is able to detect the pairwise physical contacts of all chromosomal loci. The Hi-C data shows that chromosomes are composed of 3D compartments that range over a variety of scales. However, it is challenging to systematically detect these cross-scale structures. Most studies have therefore designed methods for specific scales to study foremost topologically associated domains (TADs) and A/B compartments. To go beyond this limitation, we tailor a network community detection method that finds communities in compact fractal globule polymer systems. Our method allows us to continuously scan through all scales with a single resolution parameter. We found: (i) polymer segments belonging to the same 3D community do not have to be in consecutive order along the polymer chain. In other words, several TADs may belong to the same 3D community. (ii) CTCF proteins—a loop-stabilizing protein that is ascribed a big role in TAD formation—are correlated well with community borders only at one level of organization. (iii) TADs and A/B compartments are traditionally treated as two weakly related 3D structures and detected with different algorithms. With our method, we detect both by simply adjusting the resolution parameter. We therefore argue that they represent two specific levels of a continuous spectrum 3D communities, rather than seeing them as different structural entities.

---

## Introduction

Data from experiments that detect physical contacts between DNA loci in the nucleus, such as Hi-C [1, 2], show that DNA in the nucleus is not a randomly folded polymer. Rather, across cell types and organisms, Hi-C experiments reveal that chromosomes are built up by a network of three dimensional (3D) compartments.

At the mega( $10^6$ )-base-pair scale, two types of coexisting structures stand out. In one, all chromosome loci seem to belong to one of the two so-called A/B compartments, where the chromatin in one compartment is generally more open, accessible, and actively transcribed than the other. In the second type, linear subsections of the genome assemble into topological domains [3, 4], often referred to as topologically associated domains (TADs) [2–4]. Plotting Hi-C data as a 2D heat map, TADs show up as local regions with sharp borders with more internal than external contacts. The positions of these borders are correlated with several genetic processes, such as transcription, localization of some epigenetic marks, and DNA-binding profiles of several proteins—most notably CTCF and cohesin [3, 4].

The methods that detect TADs are not the same as those that find A/B compartments. Therefore, TADs and A/B compartments are treated as different 3D structures that are only weakly related to each other. Just as for TADs, there are several algorithms tailored for detecting A/B compartments [1, 5], each with their strengths and weaknesses.

To algorithmically detect TAD-like structures, there exists by now a menagerie of network [6–10] and clustering approaches [11–17]. Arguably these methods yield overlapping results, but it is unclear by how much. In particular, some methods cannot deal with TAD-within-TAD hierarchies that become apparent when zooming in TADs in highly resolved Hi-C maps. This means that there is not a universal definition for what a TAD really is.

Some network approaches are based on community detection methods that are related to what we use here. In Ref. [7], the authors suggest a method based on the stochastic block model [16, 17], which is another side of the network community detection field compared to the modularity maximization method that we use here (but as shown recently [18], they are connected). However, there are some limitations in their approach. For example, they binarize the Hi-C data (‘0’ or ‘1’ with a rather arbitrarily chosen thresholds) thereby discarding contact frequency variations in the Hi-C data. Furthermore, there is no comparative study connecting their communities to biological factors or any mechanistic models. Reference [8] takes a step in this direction, but the method to detect the TADs itself relies on biological factor data and nontrivial threshold criteria.

To overcome some of these problems, we start by acknowledging that the internal 3D organization of the chromosomes is richer than simply TADs and A/B compartments. These are just two examples. To capture this, we develop a new network-based method that allows us to scan through 3D structures on all scales with the help of a resolution parameter. In particular, our approach is based on the GenLouvain method, originally designed for network community detection. For a specific value of the resolution parameter, the method finds the optimal community structure with respect to a null model of the network that has to be specified beforehand. Based on the physics of compact polymer globules, we put forward a null model that is consistent with average contact probabilities in real Hi-C data [1]. This goes beyond previous Louvain-like studies [14, 15] that treat the Hi-C data as a network with random connections.

Furthermore, most studies, such as Refs. [14, 15], treat TADs as linear contiguous sequences of chromatin. This restriction overrides the GenLouvain algorithm’s ability to find the (not necessarily contiguous) optimal community structure in the data set [19]. We remove this restriction in our study. Therefore, to reduce confusion, we will not use

---

the term TAD, but rather the *3D community* for the cluster of nodes that comes out of the GenLouvain algorithm since they are not necessarily linear contiguous sequences.

## Community detection with the GenLouvain method

We use the GenLouvain algorithm [20] to detect communities in the Hi-C maps (this is an extension of the original Louvain method [21]). This algorithm gives us the possibility to find communities at several scales with a single resolution parameter  $\gamma$ . Contrasting other methods with similar features, the spectrum of communities that we detect is not necessarily hierarchical or nested, as in e.g. Refs. [8, 22, 23]. Instead, two different values of  $\gamma$  give two different collections of communities, and these do not necessarily have anything to do with each other.

To find the communities, the GenLouvain method tries putting the nodes into different communities to maximize the so-called modularity function  $Q$ . This function quantifies by how much more dense the connections are within the communities compared to what they would be in a particular type of network, say a random network. GenLouvain's modularity function is

$$Q = \frac{1}{2m} \sum_{i \neq j} [(A_{ij} - \gamma P_{ij}^{\text{null}}) \delta(g_i, g_j)] , \quad (1)$$

where the sum runs over all nodes in the network, in our case genomic loci, and  $A_{ij}$  is the pairwise number of contacts between all node pairs  $i$  and  $j$  ( $A_{ij}$  is the adjacency matrix in standard network terminology). Furthermore,  $P_{ij}^{\text{null}}$  is the null-model term that is network-type-specific, and the difference  $A_{ij} - P_{ij}^{\text{null}}$  therefore measures how strongly nodes  $i$  and  $j$  are connected in the real network, compared to how strongly we expect them to be given  $P_{ij}^{\text{null}}$ . Finally,  $\delta(g_i, g_j)$  is the Kronecker delta that is unity only if nodes  $i$  and  $j$  belong to the same community (otherwise it is zero), and  $m$  is a normalization factor so that  $Q$  goes between  $-1$  and  $+1$ .

One of the most popular choices for  $P_{ij}^{\text{null}}$  is the Newman-Girvan (NG) null-model term for a random network,  $P_{ij}^{\text{NG}} = k_i k_j / (2m)$  [24]. For a unweighted network where  $A_{ij}$  is either zero or one,  $k_i$  and  $k_j$  are the number of links for nodes  $i$  and  $j$  ( $k_i = \sum_j A_{ij}$ ). Simply put, the NG null-model assumes that the probability that  $i$  and  $j$  are connected is proportional to the product of their number of links. The same interpretation holds for weighted networks where  $k_i$  becomes the sum of weights on the edges connected to  $i$  ("strength" in network terminology).

However, the NG null-model is too a rough approximation to find communities in Hi-C maps, because it does not obey well established contact patterns that we know exist in DNA, or in fact any polymer system. For example, DNA is a long polymer where nodes are arranged in a linear sequence and then folded in 3D. This sets limitations for how frequently two pieces of DNA, or nodes, can join in 3D space (this is usually not a restriction in most networks). As was first discovered in Ref. [1], and many papers thereafter [25, 26], the contact probability between two nodes  $i$  and  $j$  decays as a power-law with the linear distance between them, that is  $\propto |i - j|^{-\alpha}$ . Based on this, we propose the following null-model:

$$P_{ij}^{\text{FG}} = \frac{2m k_i k_j |i - j|^{-\alpha}}{\sum_{i' \neq j'} k_{i'} k_{j'} |i' - j'|^{-\alpha}} . \quad (2)$$

The value of the decay exponent  $\alpha$  is debatable, but we use  $\alpha = 1$ . There are two main reasons. First, at the mega-base-pair scale of human DNA, the Hi-C data suggests that it is close to one [1] ( $\alpha$  is also close to one in mice [26]). Second, in the next section

we will study community detection in the fractal globule polymer (hence the superscript FG in  $P_{ij}^{\text{FG}}$ ) where we know that  $\alpha = 1$  [27, 28]. Nonetheless, we point out that our method does not rely on this choice, and  $\alpha$  is in principle a free parameter.

## 3D communities in fractal globules

Before we investigate the human Hi-C data, we wish to better understand the explicit 3D structures that our community detection method picks up. To do this, we use computer-generated fractal globule polymers (denoted by the “crumpled globule” in the original article [29]). This is a compact polymer that mimics the large scale structure of human chromosomes, in particular the scaling relations of the end-to-end distance and contact frequency [1]. The advantage of this approach is that we have the explicit 3D coordinates for every part of the polymer (because we made it), which allows us to visualize and analyze the 3D structure of the communities that we detect. For the Hi-C map, we only have pairwise contact frequencies and the 3D structure is precisely what we would like to know.

### Generating fractal globules with the conformation-dependent polymerization algorithm

We generate an ensemble of fractal globule polymers using the conformation-dependent polymerization (CDP) model [27]. In a nutshell, this is a Monte Carlo method that produces a fractal globule by simulating a biased random walk on lattice where the propagation probability depends on the entire walk’s trajectory over the lattice [27]. This yields on-lattice space-filling polymers. To generate off-lattice fractal globules, the structure is randomized with simulated annealing where the position of a monomer is randomly displaced under the constraint of a fixed inter-monomer distance. With properly chosen parameters<sup>1</sup>, the CDP method produces a fractal globule with contact frequency (probability) that decays as  $\sim s^{-1}$  (as it should [28]), where  $s$  is the contour distance along the polymer. This result is consistent with the Hi-C data for the human genome at the mega-base-pair scale [1]. We show a realization of a CDP in Fig. 1(a).

From every simulated CDP polymer, we construct a contact map by counting the number of contact events between polymer beads  $i$  and  $j$ . The contact refers to the case where the Euclidean distance between two beads are shorter than three lattice spacings. To obtain good statistics, we first generate an on-lattice polymer, and then during the annealing stage we register all contacts in  $10^3$  random variations of the on-lattice structure. In addition, we have confirmed that different threshold values for what we consider as a contact do not qualitatively alter our results presented below. Just as in the Hi-C experiments, in the final step we normalize the contact map with the KR-norm [30] so that each row and column sums to unity.

As a reference case, we use the equilibrium globule. This is a self avoiding polymer in a closed spherical volume. When we generate equilibrium globules, we contain it in a volume with the same diameter as the fractal globules’ radius of gyration.

### Structure of 3D communities in fractal globules

Figure 1(b) shows the contact map for one simulated CDP, where higher pixel intensity means a larger number of contacts. Just as in real Hi-C maps, the simulated map contains locally concentrated contact domains along the diagonal, that is, along the polymer chain. To find these domains algorithmically, we put the contact map into our

<sup>1</sup>To use the notation from Ref. [27], we use the relation  $p \propto (1 + An)$  with  $A = 10^4$  for an unoccupied site and  $p$  to an occupied site is given by  $\epsilon = 10^{-4}$ .

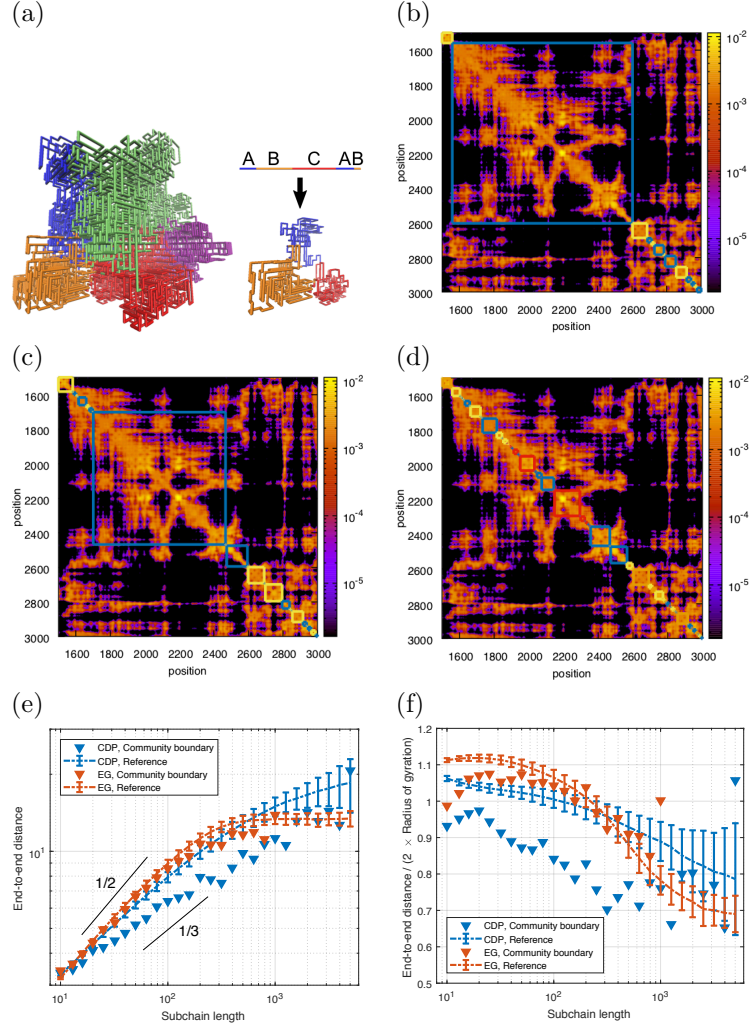


**Fig 1. 3D communities in simulated fractal globules.** (a, left) The 3D representation of fractal globule from the CDP algorithm. The colors highlight communities that we detect using Eq. (2),  $\gamma = 0.6$ . (a, right) The communities are not contiguous: the small globule is a subsection of the lower left part of polymer, and the stretched version shows the alternating communities (ABCAB). (b)-(d) The contact maps of simulated fractal globules after KR-normalization, with various resolution parameters: (b)  $\gamma = 0.4$ , (c)  $\gamma = 0.6$ , and (d)  $\gamma = 0.8$ . To show non-contiguous communities, we superimpose them as the squares; the same color indicates that they belong to the same 3D community. (e) The end-to-end distance for the fractal (FG, blue) and the equilibrium globules (EG, red) averaged over 200 polymer realizations. The triangles denote the end-to-end distance for community boundaries, and dashed lines represent the chain as a whole. To find the communities, we use  $\gamma = 0.4$ . The data are obtained from the simulation of 200 sample globules for each polymer model. The error bars show the standard error of the mean, and the two guided slopes ( $1/2$  and  $1/3$ ) show the known scaling of equilibrium and fractal globules at intermediate length scales. (f) The same data as in the panel (e), where we scale the vertical axis with the radius of gyration.

modified GenLouvain method. By varying the resolution parameter  $\gamma$ , we detect communities on various scales. On top of the contact map in Figs. 1(b)–(d), we overlay examples of 3D communities for  $\gamma = 0.4$  (b),  $\gamma = 0.6$  (c), and  $\gamma = 0.8$  (d), where the boxes represent community boundaries. Now we ask what the 3D structure of these communities is, and if and how they are different from the fractal globule polymer as a whole.

Contrasting preconceived ideas about TADs, we find that 3D communities do not have to be composed of a contiguous polymer segment. Rather, linearly distant parts of the polymer can be folded in 3D and form a community. We show this in Fig. 1(a, left), where we mark the polymer segments belonging to the same community with the same color ( $\gamma = 0.6$ ). In Fig. 1(a, right), we cut out a subsection with three communities and stretch it out. Labeling the communities as A, B, and C, they are clearly ordered in a non-contiguous sequence: they appear as A-B-C-A-B rather than A-B-C.

Furthermore, because of the above-average contact frequencies inside a community, we would like to quantify how their 3D structure differs from the fractal globule polymer as a whole. To do this, we examine the scaling relation of the end-to-end distance—the Euclidean distance between the two boundary monomers defining that (contiguous) community—with respect to the subchain length  $s$ .

In Fig. 1(e), we show this relation for the community subchains (the blue triangles) and for all subchains (the blue dashed lines). It shows that the end-to-end distance for the entire globule grow as  $\sim s^{1/3}$ , as is expected for a space-filling curve (deviations for large- $s$  comes from finite-size effects and insufficient statistics). For the communities, we notice that the end-to-end distances are systematically smaller than for a randomly chosen subchains. Our simulations even suggests that the scaling exponent is smaller than  $1/3$ . Overall, this shows that our method detects 3D communities are compact substructures of the fractal globule.

For comparison, we made the same analysis for the equilibrium globule (EG). In Fig. 1(e), we see that the end-to-end distance for our 3D communities and all subchains have the same scaling:  $\sim s^{1/2}$  for  $s \lesssim N^{2/3}$  and  $\sim s^0$  for  $s \gtrsim N^{2/3}$ , as we expect from an  $N$  monomer ideal chain.

To explain what TADs are in Hi-C data, several groups have suggested that a large fraction of them are simple loops. To see if the 3D communities we detect also are loops, we measured the absolute distance between two boundary monomers relative to the community’s size (measured by the radius of gyration). If the communities are loops, the distance should be close to zero. In Fig. 1(f), we plot the ratio of the end-to-end distance to the corresponding radius of gyration the subchains. It is clear that this ratio is smaller for the community subchains (the blue triangles) than a random subchain in the fractal globule (the blue dashed line). This implies that the two boundary monomers have a shorter end-to-end distance than on average, but the 3D communities are not simple loops. This observation suggests the need for loop-stabilizing proteins to form loops, such as CTCF.

## Community detection for the Hi-C map

After validating our method with the simulated polymer model, we proceed to analyze Hi-C data from human cells [2]. The data comes in the form of matrices where each entry represents the number contacts between two chromosome loci  $i$  and  $j$ . As is standard in the field, we normalized the data with the KR-norm [30] which balances the matrix such that every row and column sum to unity (we also used the KR-norm for the fractal globule contact data). The data is available in various resolutions, from  $10^3$  base pairs (1 kbp) to  $10^6$  base pairs (1 Mbp), but we used 100 kbp which is the scale where both TADs and A/B compartments can be detected [2].

In Figs. 2(a)–(c), we show that our algorithm detects differently sized contiguous blocks, or TADs, along the chromosome arms as we change the resolution parameter  $\gamma$ . Similar to the simulated data, it is clear that several TADs form 3D communities. To investigate how these TADs correspond to TADs defined in other studies, we compared the border locations of each contiguous block to TAD borders defined by Rao *et al.* [2] (the group that produced the dataset we use in this study) in Fig. 2(d). At  $\gamma \approx 0.7$ , about 70% of the borders overlap. Moreover, several studies have shown that binding sites for the insulator protein CTCF are strongly correlated with TAD borders (e.g., in Ref. [3]). We therefore check the overlap between CTCF binding sites (mapped by ENCODE [31]) and all borders at different  $\gamma$  values. We note that CTCF has the highest overlap also at  $\gamma \approx 0.7$  (Fig. 2(d)).

As we discussed in the introduction, there are different algorithms that detect TADs. However, regardless of the definition that is used, the TADs that come out have substructures that we can interpret as TAD-within-TADs [12] with new sets of borders. Our algorithm let researchers scan through all these TAD-within-TADs. According to Fig. 2(d), CTCF correlate well with TAD borders at  $\gamma \approx 0.7$ . This level also coincides with TADs from Ref. [2]. Our method opens the possibility to investigate which family of proteins is important for different hierarchical levels. This is not pursued further here, and left for future studies.

We next investigate properties of the 3D communities. First, we count the number of communities and average number of TADs within each community at different  $\gamma$  (Fig. 2(e)) as well as their localization along the chromosome arms (Fig. 2(f)). The highest number of TADs/community is when  $\gamma = 0.6$  and  $\gamma = 0.75$  (about 17 TADs/community). Interestingly, for  $\gamma < 0.6$ , the chromosome consists of only two communities (but with several TADs within them).

Second, we map gene activity within each community using RNA-seq data from ENCODE [32] (GEO Acc. Nr: GSE88583). In Figs. 2(g)–(i) and Supplementary Figs. S1–S4, we show the average coverage of RNA-seq reads within communities for different  $\gamma$ . At small  $\gamma$  values where only two communities are defined, one community is clearly more active than the other. The active and less active communities are then split up into smaller communities as  $\gamma$  increases. Already in the original Hi-C paper by Lieberman-Aiden *et al.* [1], they used principal component analysis on the Hi-C data to partition the chromosomes into two classes. Denoting them by A/B compartments, they found that the A compartment contains transcriptionally active chromatin, whereas the B compartment is less active. It is striking and unprecedented that by tuning a single parameter, we detect both TADs and A/B compartments with the same algorithm. We therefore argue that TADs and A/B compartments are not two conceptually different organizational structures in the nucleus, but rather different ends of the same organizational spectrum.

## Conclusions and outlook

From Hi-C experiments, it is clear that inter-phase chromosomes are built up by a network of 3D compartments on various scales—from kilo( $10^3$ )-base-pair sized loops to mega( $10^6$ )-base-pair sized 3D structures. This pattern is consistent across organisms and cell types. To let researchers scan through the spectrum of 3D compartments, we have tailored the GenLouvain community detection method to find 3D communities in fractal globule polymer systems. Apart from verifying our method on computer-generated polymers, we have applied it to analyze human Hi-C data. First, we have found that chromatin segments belonging to the same 3D community do not have to be in next to each other along the DNA. In other words, several TADs can belong to the same 3D community. Second, we have found that CTCF proteins—a

---

loop-stabilizing protein that is ascribed a big role in TAD formation—are only correlated well with community borders at one level of organization. It remains to find what other factors are important at higher or lower levels. Third, just by adjusting a single parameter ( $\gamma$ ), our method picks up the two most prominent 3D compartments, TADs and A/B compartments, which are traditionally treated as two weakly related 3D structures and detected with different algorithms. Rather than seeing them as different, our work put them on an equal footing, and we argue that they represent two ends of a continuous spectrum of 3D communities of different sizes.

## Supporting information

**Fig. S1. Differential RNA expression levels for different communities.** We present the results in Figs. 2(g)–(i) corresponding to various values of  $\gamma$  for chromosomes 1–6, only for the largest and second largest communities. For visualization, we shift the box plots slightly to the left for the largest community and right for the second largest community for each of the  $\gamma$  values.

**Fig. S2. Differential RNA expression levels for different communities.** We present the results in Figs. 2(g)–(i) corresponding to various values of  $\gamma$  for chromosomes 7–12, only for the largest and second largest communities. For visualization, we shift the box plots slightly to the left for the largest community and right for the second largest community for each of the  $\gamma$  values.

**Fig. S3. Differential RNA expression levels for different communities.** We present the results in Figs. 2(g)–(i) corresponding to various values of  $\gamma$  for chromosomes 13–18, only for the largest and second largest communities. For visualization, we shift the box plots slightly to the left for the largest community and right for the second largest community for each of the  $\gamma$  values.

**Fig. S4. Differential RNA expression levels for different communities.** We present the results in Figs. 2(g)–(i) corresponding to various values of  $\gamma$  for chromosomes 19–22 and X, only for the largest and second largest communities. For visualization, we shift the box plots slightly to the left for the largest community and right for the second largest community for each of the  $\gamma$  values.

## Acknowledgments

The authors thank Rajendra Kumar for fruitful discussion and the practical help in various data processing throughout our work. This work was supported by the National Research Foundation (NRF) of Korea (No. 2016K2A9A2A12003797), and the Knut and Alice Wallenberg foundation (grant number 2014-0018, to EpiCoN, co-PI: PS). S.H.L. was also supported by Gyeongnam National University of Science and Technology Grant in 2018–2019 and the NRF of Korea (No. 2018R1C1B5083863).

## References

1. Lieberman-Aiden E, van Berkum NL, Williams L, Imakaev M, Ragoczy T, Telling A, et al. Comprehensive mapping of long-range interactions reveals folding principles of the human genome. *Science*. 2009; 326: 289–293.  
<https://doi.org/10.1126/science.1181369> PMID: 19815776

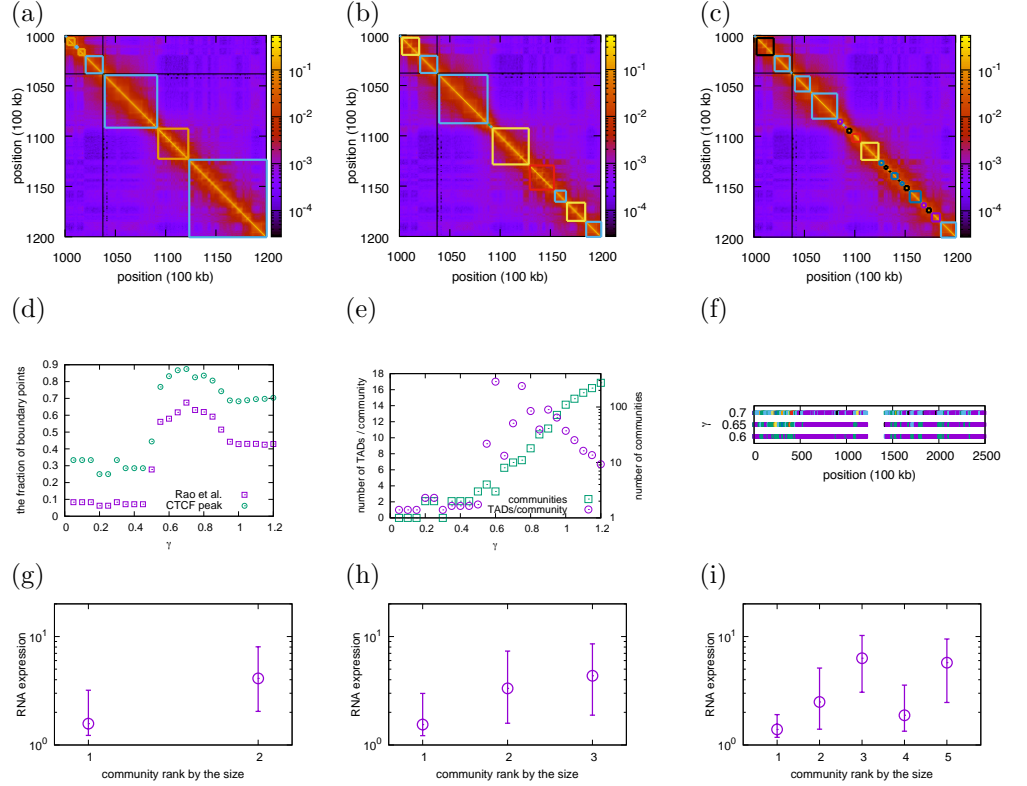


**Fig 2. 3D communities in real Hi-C data (chromosome 1).** (a)–(c): Normalized Hi-C data with squares showing the structure of 3D communities. The black regions are the unmappable regions. The resolution parameter ranges from  $\gamma = 0.6$  (a),  $\gamma = 0.7$  (b), and  $\gamma = 0.8$  (c). As in Figs. 1(b)–(d), we assign the same colors to those squares that belong to the same 3D community. It is clear that they are not contiguous sequences. (d) The fraction of community boundary points predicted by our method that coincide with the ones in Rao *et al.* [2] (the squares), and binding positions for CTCF (the circles) for different values of  $\gamma$ . (e) The average number of TADs for each community, and the number of communities as functions of  $\gamma$ . (f) The community division along chromosome 1 for three different values of  $\gamma$ . The purple squares represent the largest community in the panels (g)–(i), while the other colors indicate smaller communities. (g)–(i) Communities' gene activity sorted by their relative size for different values of  $\gamma$ : (g)  $\gamma = 0.6$ , (h)  $\gamma = 0.65$ , and (i)  $\gamma = 0.7$ . The circles show the median RNA expression levels, and vertical lines are quartiles. We omit communities that are smaller than 50 nodes to ignore too small communities. We find the communities using Eqs. (1) and (2).

- 
2. Rao SSP, Huntley MH, Durand NC, Stamenova EK, Bochkov ID, Robinson JT, et al. A 3D map of the human genome at kilobase resolution reveals principles of chromatin looping. *Cell*. 2014; 159: 1665–1680.  
<https://doi.org/10.1016/j.cell.2014.11.021> PMID: 25497547
  3. Dixon JR, Selvaraj S, Yue F, Kim A, Li Y, Shen Y, et al. Topological domains in mammalian genomes identified by analysis of chromatin interactions. *Nature*. 2012; 485: 376–380. <https://doi.org/10.1038/nature11082> PMID: 22495300
  4. Nora EP, Lajoie BR, Schulz EG, Giorgetti L, Okamoto I, Servant N, et al. Spatial partitioning of the regulatory landscape of the X-inactivation centre. *Nature*. 2012; 485: 381–385. <https://doi.org/10.1038/nature11049> PMID: 22495304
  5. Dixon JR, Jung I, Selvaraj S, Shen Y, Antosiewicz-Bourget JE, Lee AY, et al. Chromatin architecture reorganization during stem cell differentiation. *Nature*. 2015; 518: 331–336. <https://doi.org/10.1038/nature14222> PMID: 25693564
  6. Boulos RE, Arneodo A, Jensen P, Audit B. Revealing long-range interconnected hubs in human chromatin interaction data using graph theory. *Phys Rev Lett*. 2013; 111: 118102. <https://doi.org/10.1103/PhysRevLett.111.118102> PMID: 24074120
  7. Cabrereros I, Abbe E, Tsirigos A. Detecting community structures in Hi-C genomic data. *IEEE 2016 Annual Conference on Information Science and Systems*. 2016; 584. <https://doi.org/10.1109/CISS.2016.7460568>
  8. Wang WXR, Sarkar P, Ursu O, Kundaje A, Bickel PJ. Network modelling of topological domains using Hi-C data. e-print arXiv:1707.09587.  
<https://arxiv.org/abs/1707.09587>
  9. Sarnataro S, Chiariello AM, Esposito A, Prisco A, Nicodemi M. Structure of the human chromosome interaction network. *PLOS ONE*. 2017; 12: e0188201.  
<https://doi.org/10.1371/journal.pone.0188201> PMID: 29141034
  10. Belyaeva A, Venkatachalapathy S, Nagarajan M, Shivashankar GV, Uhler C. Network analysis identifies chromosome intermingling regions as regulatory hotspots for transcription. *Proc Natl Acad Sci USA*. 2017; Early Edition.  
<https://doi.org/10.1073/pnas.1708028115> PMID: 29229825
  11. Yu W, He B, Tan K. Identifying topologically associating domains and subdomains by Gaussian Mixture model And Proportion test. *Nat Commun*. 2017; 8: 535. <https://doi.org/10.1038/s41467-017-00478-8> PMID: 28912419
  12. Identification of hierarchical chromatin domains, Weinreb, Caleb and Raphael, Benjamin J, *Bioinformatics*, 32:(11): 1601–1609, 2015,  
<https://doi.org/10.1093/bioinformatics/btv485>
  13. Haddad N, Vaillant C, Jost D. IC-Finder: inferring robustly the hierarchical organization of chromatin folding. *Nucleic Acids Res*. 2017; 45: e81.  
<https://doi.org/10.1093/nar/gkx036> PMID: 28130423
  14. Yan KK, Lou S, Gerstein M. MrTADFinder: A network modularity based approach to identify topologically associating domains in multiple resolutions. *PLOS Comput Biol*. 2017; 13: e1005647.  
<https://doi.org/10.1371/journal.pcbi.1005647> PMID: 28742097

- 
15. Norton HK, Emerson DJ, Huang H, Kim J, Titus KR, Gu S, et al. Detecting hierarchical genome folding with network modularity. *Nat Methods*. 2018; Advanced Online Publication. <https://doi.org/10.1038/nmeth.4560>
  16. Ball B, Karrer B, Newman MEJ. Efficient and principled method for detecting communities in networks. *Phys Rev E*. 2011; 84: 036103. <https://doi.org/10.1103/PhysRevE.84.036103> PMID: 22060452
  17. Gopalan PK, Blei DM. Efficient discovery of overlapping communities in massive networks. *Proc Natl Acad Sci USA*. 2013; 110: 14534–14539. <https://doi.org/10.1073/pnas.1221839110> PMID: 23950224
  18. Newman MEJ. Equivalence between modularity optimization and maximum likelihood methods for community detection. *Phys Rev E*. 2016; 94: 052315. <https://doi.org/10.1103/PhysRevE.94.052315> PMID: 27967199
  19. Porter MP, Onnela JP, Mucha PJ. Communities in networks. *Not Am Math Soc*. 2009; 56: 1082–1092, 1164–1166. <https://people.maths.ox.ac.uk/~porterm/papers/comnotices.pdf>; Fortunato S. Community detection in graphs. *Phys Rep*. 2010; 486: 75–174. <https://doi.org/10.1016/j.physrep.2009.11.002/>
  20. Jutla IS, Jeub LGS, Mucha PJ. Generalized Louvain method for community detection implemented in MATLAB (GenLouvain 2.0). Available at <http://netwiki.amath.unc.edu/GenLouvain/GenLouvain>. 2011–2014.
  21. Blondel VD, Guillaume J-L, Lambiotte R, Lefebvre E. Fast unfolding of communities in large networks. *J Stat Mech Theory Exp*. 2008; 2008: P10008. <https://doi.org/10.1088/1742-5468/2008/10/P10008>
  22. Fraser J, Ferrai C, Chiariello AM, Schueler M, Rito T, Laudanno G, et al. Hierarchical folding and reorganization of chromosomes are linked to transcriptional changes in cellular differentiation. *Mol Syst Biol*. 2015; 11: 852. <https://doi.org/10.15252/msb.20156492> PMID: 26700852
  23. Bianco S, Chiariello AM, Annunziatella C, Esposito A, Nicodemi M. Predicting chromatin architecture from models of polymer physics. *Chromosome Res*. 2017; 25: 25–34. <https://doi.org/10.1007/s10577-016-9545-5> PMID: 28070687
  24. Newman MEJ, Girvan M. Finding and evaluating community structure in networks. *Phys Rev E*. 2004; 69: 026113. <https://doi.org/10.1103/PhysRevE.69.026113> PMID: 14995526
  25. Burton JN, Liachko I, Dunham MJ, Shendure J. Species-level deconvolution of metagenome assemblies with Hi-C-based contact probability maps. *G3 (Bethesda)*. 2014; 4: 1339–1349. <https://doi.org/10.1534/g3.114.011825> PMID: 24855317
  26. Zhang Y, McCord RP, Ho YJ, Lajoie BR, Hildebrand DG, Simon AC, et al. Spatial organization of the mouse genome and its role in recurrent chromosomal translocations. *Cell*. 2012; 148: 908–921. <https://doi.org/10.1016/j.cell.2012.02.002> PMID: 22341456
  27. Tamm MV, Nazarov LI, Gavrilov AA, Chertovich AV. Anomalous diffusion in fractal globules. *Phys Rev Lett*. 2015; 114: 178102. <https://doi.org/10.1103/PhysRevLett.114.178102> PMID: 25978267

- 
28. Mirny LA. The fractal globule as a model of chromatin architecture in the cell. *Chromosome Res.* 2011; 19: 37–51.  
<https://dx.doi.org/10.1007/s10577-010-9177-0> PMID: 21274616
  29. Grosberg A, Rabin Y, Havlin S, Neer A. Crumpled globule model of the three-dimensional structure of DNA. *EPL.* 1993; 23: 373–378.  
<https://doi.org/10.1209/0295-5075/23/5/012>
  30. Knight PA, Ruiz D. A fast algorithm for matrix balancing. *IMA J Numer Anal.* 2013; 33: 1029–1047. <https://doi.org/10.1093/imanum/drs019>
  31. ENCODE Project Consortium and others, An integrated encyclopedia of DNA elements in the human genome, *Nature* 2012; 57:7414  
<https://doi.org/10.1038/nature11247> PMID: 22955616, GEO Acc. Nr: GSM733752.
  32. The ENCODE Project Consortium. An integrated encyclopedia of DNA elements in the human genome. *Nature* 2012; 489: 57–74.  
<https://doi.org/10.1038/nature11247> PMID: 22955616

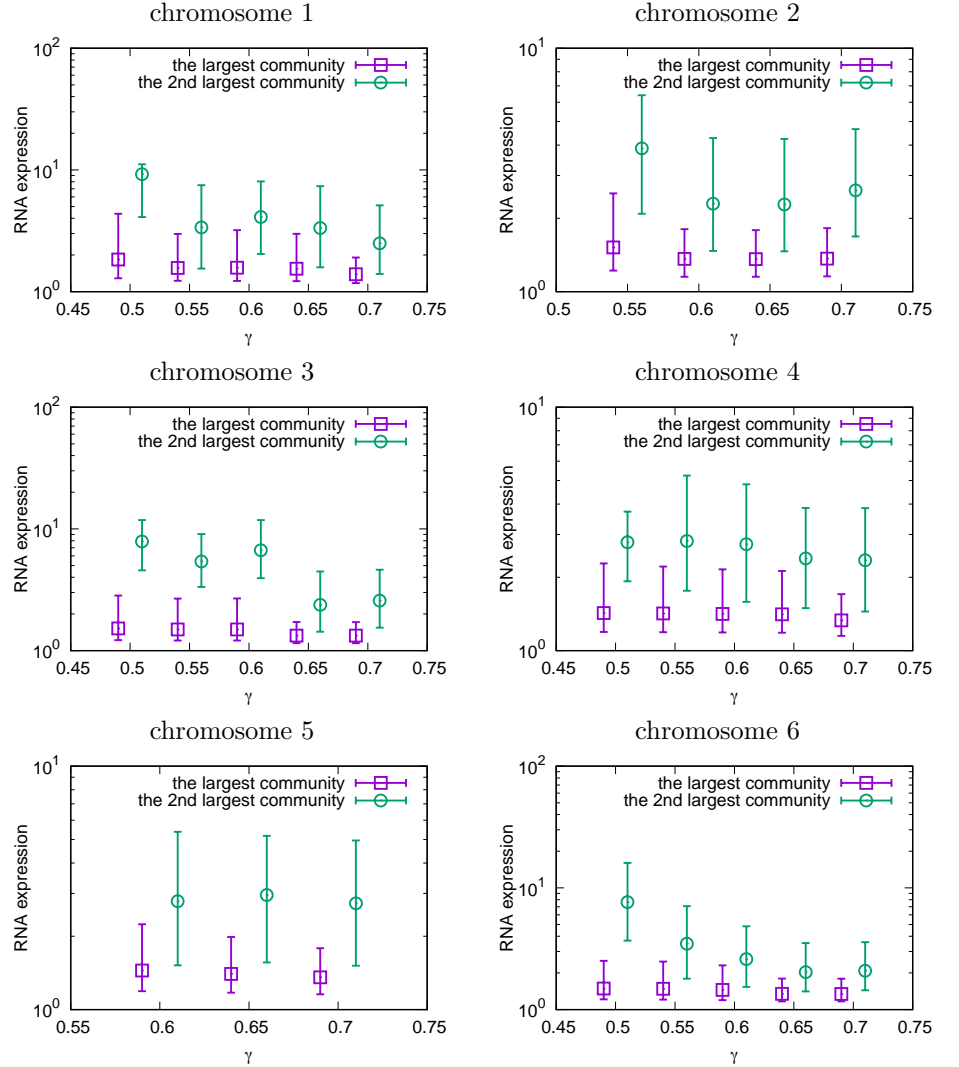


**Fig S1. Differential RNA expression levels for different communities.** We present the differential RNA expression for communities corresponding to various values of  $\gamma$  for chromosomes 1–6, only for the largest and second largest communities. For visualization, we shift the data points slightly to the left for the largest community and right for the second largest community for each of the  $\gamma$  values. The plots indicate the median values with the quartiles as the error bars.

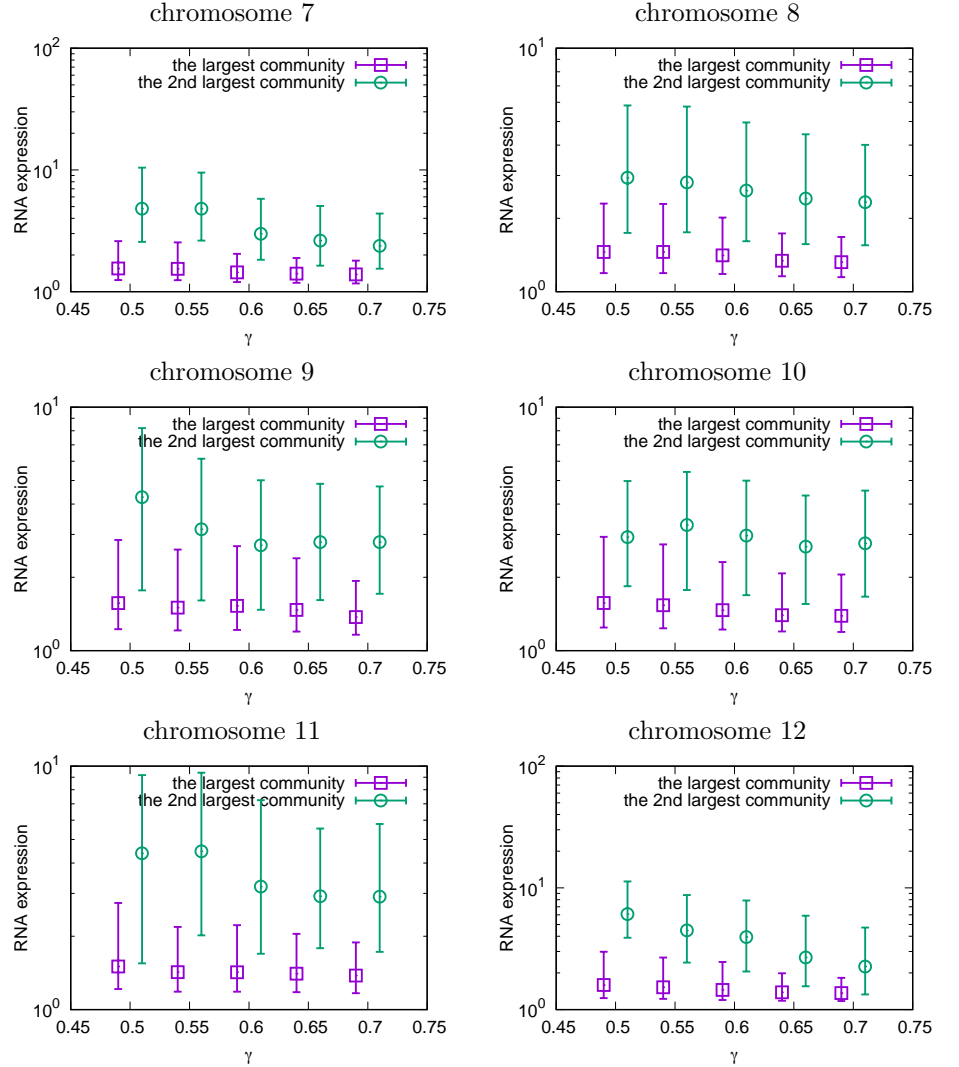


**Fig S2. Differential RNA expression levels for different communities.** We present the differential RNA expression for communities corresponding to various values of  $\gamma$  for chromosomes 7–12, only for the largest and second largest communities. For visualization, we shift the data points slightly to the left for the largest community and right for the second largest community for each of the  $\gamma$  values. The plots indicate the median values with the quartiles as the error bars.

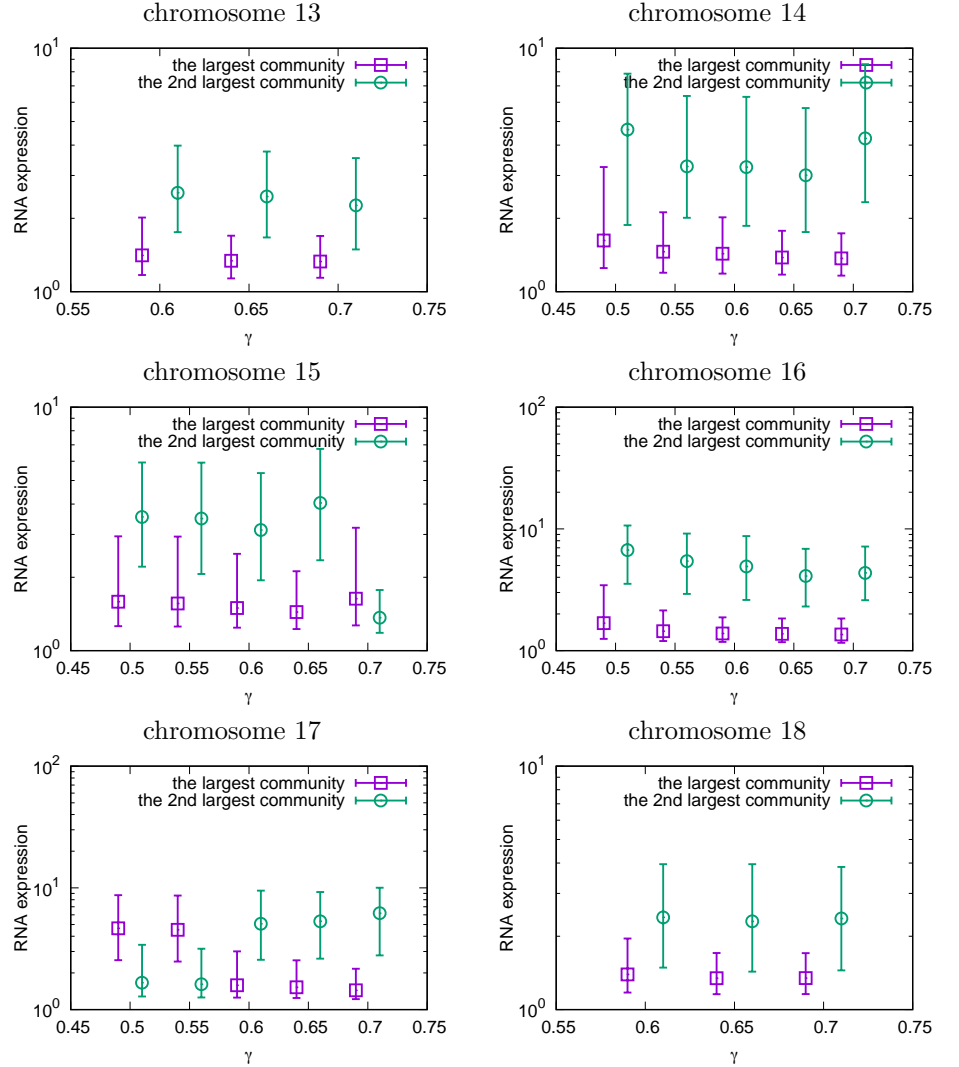


**Fig S3. Differential RNA expression levels for different communities.** We present the differential RNA expression for communities corresponding to various values of  $\gamma$  for chromosomes 13–18, only for the largest and second largest communities. For visualization, we shift the data points slightly to the left for the largest community and right for the second largest community for each of the  $\gamma$  values. The plots indicate the median values with the quartiles as the error bars.

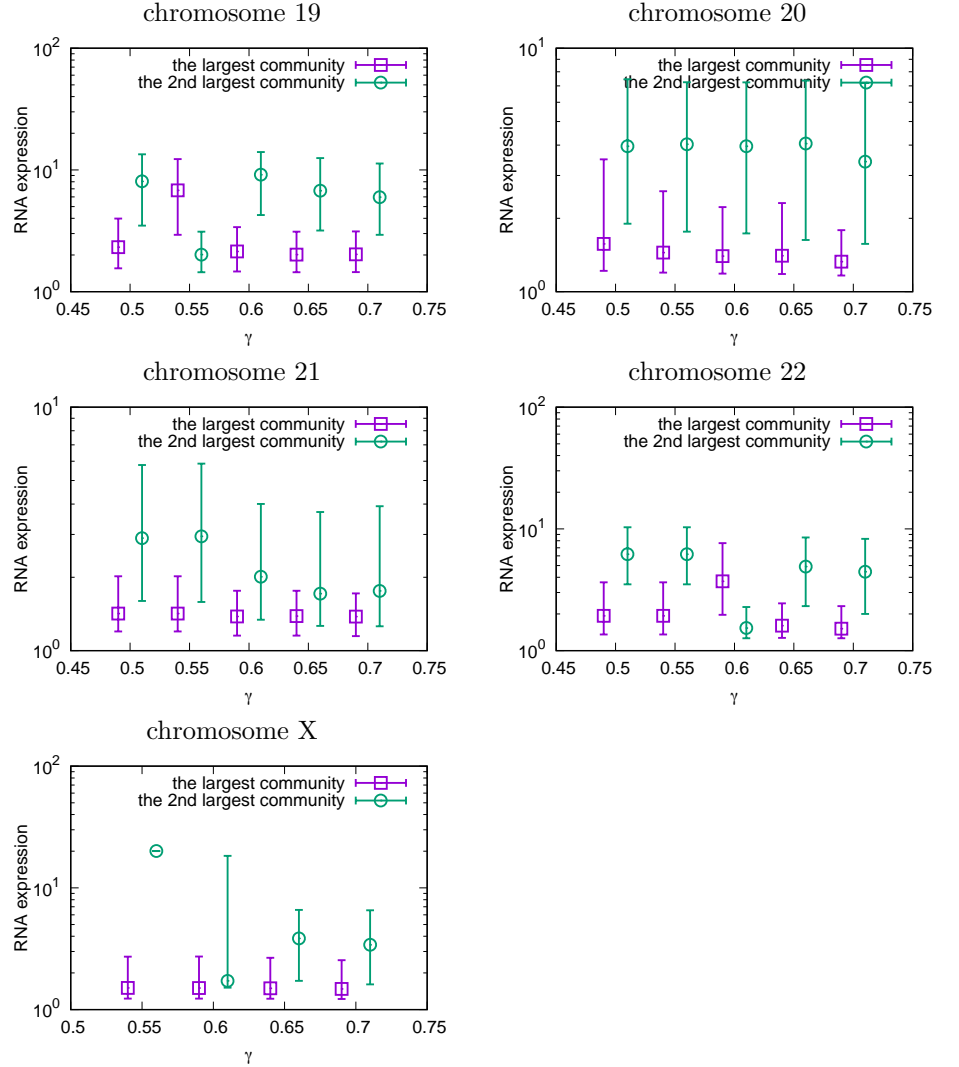


**Fig S4. Differential RNA expression levels for different communities.** We present the differential RNA expression for communities corresponding to various values of  $\gamma$  for chromosomes 19–22 and X, only for the largest and second largest communities. For visualization, we shift the data points slightly to the left for the largest community and right for the second largest community for each of the  $\gamma$  values. The plots indicate the median values with the quartiles as the error bars.